Molecular Alignment of Polymer Liquid Crystals in Shear Flows. 1. Spectrographic Birefringence Technique, Steady-State Orientation, and Normal Stress Behavior in Poly(benzyl glutamate) Solutions

K. Hongladarom and W. R. Burghardt*

Department of Chemical Engineering, Northwestern University, Evanston, Illinois 60208

S. G. Baek, S. Cementwala, and J. J. Magda

Department of Chemical Engineering, University of Utah, Salt Lake City, Utah 84112

Received August 3, 1992; Revised Manuscript Received October 27, 1992

ABSTRACT: We describe results of an experimental investigation into the orientation state of liquid crystalline solutions of poly(benzyl glutamate) under shear flow and how the microscopic structure relates to the macroscopic mechanical rheological behavior. The technique of flow birefringence was used to study the degree of molecular orientation. A spectrographic flow birefringence apparatus is described that eliminates ambiguities associated with multiple orders of retardation in birefringence measurements. The birefringence observed in textured solutions under shear flow is always less than that measured in quiescent, defect-free monodomains of the solutions. At low shear rates, the birefringence is roughly constant and in the range of 53–63% of that observed in a monodomain; there is no evidence of a low-orientation, "piled polydomain" structure. At high shear rates, the birefringence is again roughly constant and around 90% of the monodomain value. The transition between low- and high-orientation states as a function of shear rate is closely correlated with changes in sign of the first normal stress difference of these solutions, leading us to identify it as a manifestation of a transition between regimes of director tumbling at low shear rates and flow alignment at high shear rates. These observations are compared qualitatively and quantatively with predictions of the nonlinear Doi molecular model for textureless samples [Larson, R. G. *Macromolecules* **1990**, *23*, 3983] and the linear Larson and Doi tumbling polydomain model for textured samples [Larson, R. G.; Doi, M. *J. Rheol.* **1991**, *35*, 539]. An accompanying paper considers transient flow phenomena at low shear rates.

1. Introduction

The technological importance of liquid crystalline polymer solutions stems from the ability to spin ultrahigh-modulus polymer fibers from lyotropic solutions of rodlike polymers. As a consequence, the rheological behavior of polymer liquid crystals (PLC's) has been the subject of intensive investigation over the past 15 years. Since the practical utility of these materials arises from the high molecular orientation induced during fiber spinning operations, the relationship between deformation history and the resulting molecular orientation state in the solution is of central interest. The structural complexity of liquid crystalline polymer solutions introduces severe complications into these efforts. Since PLC's are anisotropic at rest, flow fields may affect orientation merely by rotating the average direction of molecular orientation (denoted by the unit vector **n**, the "director"). On the other hand, since the relaxation of the constituent macromolecules is sufficiently slow, flow fields may also perturb the degree of molecular orientation at a microscopic level, giving rise to nonlinear viscoelastic behavior. Finally, PLC's generally exhibit a defect-ridden textured structure (often refered to as a "polydomain"), disrupting the molecular orientation over a length scale on the order of microns. The rheological implications of texture are not yet fully understood; however, elastic effects associated with spatial inhomogeneity of the director field (distortional or Frank elasticity) are believed to play a central role in the relaxation behavior observed in PLC solutions at low shear rates.

Recent work uniformly suggests that the relationship between shear flow and molecular orientation is very complicated. In the limit of low shear rates, it has been shown experimentally in two systems that shear flow induces tumbling of the liquid crystal director.[1,2] Tumbling may be predicted by the linear continuum theory of Leslie and Ericksen,[3] provided certain values of the phenomenological Leslie coefficients are chosen. In the absence of either distortional or nonlinear viscoelastic effects, the tumbling orbits executed by the director are equivalent to Jeffery orbits of suspension hydrodynamics.[4] However, in a textured PLC environment it is expected that tumbling would introduce severe distortions in the director field, where the resulting Frank elastic torques on the director would frustrate indefinite tumbling, and the excess elastic energy associated with flow-induced distortions would provide the driving force for relaxation processes such as elastic recoil and stress relaxation. Burghardt and Fuller argued that the balance between viscous and elastic torques is determined by the texture length scale, a, and characterized by a local Ericksen number, $Er = \alpha\dot{\gamma}a^2/K$, where α is a characteristic viscosity, K is an elastic constant, and $\dot{\gamma}$ is the shear rate.[5] Comparisons of a range of transient flow behavior with idealized Leslie–Ericksen model calculations suggest that the texture length scale is refined in response to increase shear rate, as a means of limiting flow-induced distortional energy so that the texture-based Ericksen number is constant, resulting in a scaling $a \sim \dot{\gamma}^{-1/2}$. Similar scaling laws had been previously proposed from a variety of dimensional arguments.[6-8] Direct evidence of texture refinement is provided by microscopic visualization[9-12] as well as the wavelength dependence of anisotropic light scattering.[1] In addition, this relationship predicts a scaling law for processes associated with director field relaxation that has been intensively studied by Moldenaers and Mewis[13] and Larson and Mead.[8] Recently, Larson and Doi have developed a more sophisticated model for the

* Author to whom correspondence should be addressed.

0024-9297/93/2226-0772$04.00/0

linear regime, in which the Leslie–Ericksen model is averaged over a distribution of domain orientations.[14] Their model incorporates the various scaling arguments discussed above and provides excellent qualitative prediction of transient phenomena.

The nonlinear viscoelastic behavior of PLC solutions also reflects a complex relationship between shear flow and molecular orientation. Understanding of the nonlinear regime has been significantly advanced by series of publications by Marrucci and Maffettone[15-17] and Larson[18] that have examined the Doi molecular model[19] without resort to mathematical decoupling approximations. The major successes of the Doi model, in the absence of decoupling, are (i) the correct prediction of director tumbling in the linear limit, and (ii) the correct prediction of a region of *negative* first normal stress difference at intermediate shear rates in the nonlinear regime, observed experimentally in a number of systems. Recent experiments on the second normal stress difference of sheared PLC solutions demonstrate that Doi model predictions are also qualitatively correct for this material function.[20] The predicted normal stress behavior reflects a complex interaction between shear flow and the degree of molecular orientation, associated with a transition from tumbling to steady, flow-aligning behavior as the shear rate is increased.[15-18]

In this work, we study the molecular orientation in a model PLC solution under shear flow using the technique of flow birefringence. While birefringence is ideally suited as a measure of polymer orientation, several features of PLC's make its application somewhat challenging. The major complications are that (i) PLC's are anisotropic in the *absence* of flow, making it difficult to interpret flow-induced changes in the birefringence, and (ii) the birefringence of PLC's is very large, introducing the well-known problem of multiple orders in phase retardation. Despite these difficulties, flow birefringence has been used in the past to study PLC rheology, most notably by Asada and co-workers.[21-23] We feel, however, that new opportunities exist for this type of study. The recent theoretical progress in explaining unusual macroscopic features of PLC rheology in terms of microscopic structure provides a much richer context for the interpretation of birefringence results. Furthermore, we introduce two significant innovations in flow birefringence measurements as applied to liquid crystalline polymers. First, we utilize a spectrographic technique that eliminates the problem of multiple orders in highly anistropic materials, allowing for unambiguous measurement of birefringence. Second, by measuring the birefringence of uniformly oriented monodomains of our solutions in the absence of flow, we are able to *quantitatively* determine the effect of shear flow on the degree of orientation in textured solutions and to quantitatively test specific predictions of the models discussed above. Since the normal stress behavior observed in PLC solutions is believed to reflect complex interactions between flow and molecular orientation, we have also studied the steady-state rheological behavior of several of the test solutions in detail. Prior to the presentation of our experimental results, we explore how birefringence relates to the various structural features of sheared PLC solutions and discuss theoretical predictions of what we might expect to observe. In this paper we concentrate solely on steady-state behavior; an accompanying paper discusses molecular orientation in transient flows.[24]

2. Birefringence in PLC Solutions

The maximum birefringence that can be achieved in a polymer liquid crystal solution, Δn_0, is associated with a perfect orientation of all molecules along a single direction. Provided Δn_0 is not too large, it is expected to be roughly proportional to the concentration of rodlike polymer in the solution. Nematic liquid crystals are imperfectly ordered, however, and the degree of molecular orientation is usually expressed by a scalar order parameter, S^{eq}, such that the second moment of the rod orientation probability distribution function is given by[25]

$$\langle \mathbf{uu} \rangle = \int \psi(\mathbf{u}) \mathbf{uu}\, d\mathbf{u} = S^{eq} \mathbf{nn} \tag{1}$$

Here $\psi(\mathbf{u})\, d\mathbf{u}$ represents the probability of finding a rod oriented along the direction of unit vector $\mathbf{u}$, and $\mathbf{n}$ is the director, characterizing the average direction of molecular orientation in the uniaxial, spatially homogeneous nematic. S^{eq} varies between 0 for an isotropic medium to 1 for the case of perfect orientation. Provided that the optical anisotropy is not too large, it follows that the birefringence of a uniformly oriented PLC monodomain is

$$\Delta n_{md} = S^{eq} \Delta n_0 \tag{2}$$

We describe measurements of this quantity in section 5.

Next, we imagine that the PLC is sheared in such a way that the structure remains spatially homogeneous but allow for flow to perturb the microscopic orientation state of the PLC. Under these circumstances, we generalize eq 2 to

$$\Delta n = S \delta n_0 \tag{3}$$

where S now reflects the degree of molecular orientation under flow. (Note that S in eq 3 also reflects the geometry in which the birefringence is measured. For instance, in our experiments we measure optical anisotropy in the flow–vorticity (1–3) plane; hence S is properly thought of as representing the quantity $S_{11}-S_{33}$, the anisotropy in the appropriate components of the molecular order parameter tensor.)

Finally, we account for the additional disruption in the average degree of molecular orientation associated with the presence of a "polydomain" texture. Larson and Doi introduce the concept of a *mesoscopic* order parameter, $\bar{S}$, reflecting the degree of *domain* orientation averaged over a probability distribution function of domain orientations, $\bar{\psi}(\mathbf{n})$, where $\mathbf{n}$ is the director orientation within any given domain.[14] We finally write a qualitative expression for the birefringence of a sheared, textured, PLC solution:

$$\Delta n = \bar{S}(S \delta n_0) \tag{4}$$

reflecting imperfect orientation at both the molecular (S) and mesoscopic ($\bar{S}$) levels. Our use of *two* order parameters reflecting the two levels of disordering in textured PLC's follows the spirit of the discussion by Picken and co-workers, who studied the orientation state of sheared polyaramid solutions using X-ray scattering.[12]

Equation 4 is conceptual in nature; we use it here as a basis of thinking about what we may expect to observe in various flow regimes. At low shear rates, it is reasonable to expect that the degree of molecular orientation at a microscopic level is unperturbed by the flow (see, however, the discussion in section 7.1). We would thus replace S with S^{eq} in eq 4 and attribute any reduction in flow birefringence from Δn_{md} to the effects of the distribution of domain orientations, under the generally destructive influence of director tumbling. On the other hand, at high

shear rates, the Doi model predicts a regime of flow alignment;[15,18] that is, the flow would tend to promote the *same* orientation in each "domain". Under these circumstances, we would anticipate that the mesoscopic order parameter $\bar{S} \approx 1$ and that the measured birefringence would primarily reflect flow-induced changes in the microscopic orientation state of the material, S.

The preceding discussion tacitly assumes that the bulk optical properties of a textured PLC under shear may be represented as a simple birefringent medium. This outlook naturally obscures some delicate issues related to the propagation of polarized light through media with varying optical orientation. This issue has been lucidly discussed by Amundson and co-workers in the context of "textured" block copolymers.[26] They note that along any particular light path, a change of polarization will occur as a result of the composite effect of all the "domains" through which the light has passed. Provided the number of domains is large and the effect of a single domain is small, it is reasonable to associate this polarization change with an effective average birefringence related to the average orientation as discussed above. Amundson et al. note however that the resulting light beam contains contributions from a large number of light paths.[26] Variations in effective birefringence from one path to another mean that no single polarization state characterizes the light beam. In the studies on textured block copolymers, this prevented a true extinction condition when the average birefringence was measured using a compensation technique.[26] If the domain size is small, a given light path will sample many domains, and there would be relatively little variation in effective birefringence from one path to another and consequently little "mixing" in the polarization state. Conversely, if relatively few domains are sampled, there will be substantial variations from one light path to another and a large mixing of polarizations. Our light path of 1 mm should allow a large number of domains to be sampled (≈100), so that we are confident that our measurements provide a good quantitative description of average orientation. However, under conditions where larger scale structures are present, we may expect substantial interference from this polarization mixing. These effects appear to play an important role in measurements taken following flow cessation (see accompanying paper[24]).

3. Predictions of Molecular Alignment

3.1. Nonlinear Doi Model for Textureless Samples. Our discussion of the Doi model predictions is based on the calculations of Larson.[18] While the work of Marrucci and Maffettone shows virtually identical qualitative features,[15,16] it is less well suited to the present purposes, in that their restriction of molecular orientations to two dimensions makes predictions of anisotropy in the 1-3 plane less well founded (similar considerations apply to polydomain systems, where Marrucci and Maffettone have developed a two-dimensional model[17] that is analogous to the Larson and Doi model discussed in section 3.2). Key Doi model predictions for the purpose of our discussion are (i) a series of transitions from director tumbling in the linear regime, through a wagging (frustrated tumbling) regime, to a regime of steady flow alignment as the shear rate is increased, and (ii) associated predictions of N_1 that show transitions from positive to negative and back again to positive values as the shear rate increases. The molecular origin of negative N_1 values was identified by Marrucci and Maffettone as a flow-induced *decrease* in the degree of molecular orientation.[15]

Representative results from ref 18 (courtesy of Dr. Larson) are reproduced in Figure 1, showing results of

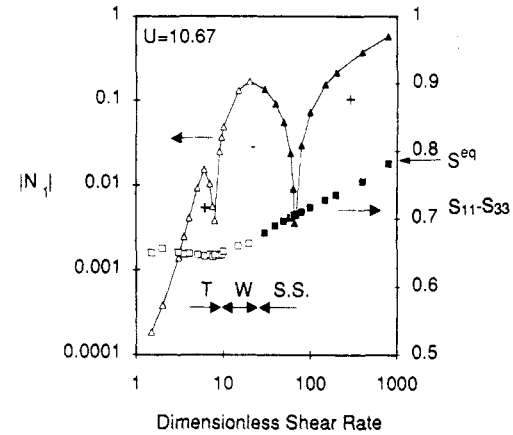

Figure 1. Predictions of dimensionless magnitude of the first normal stress difference $|N_1|$ and anisotropy in microscopic order parameter tensor $S_{11} - S_{33}$ vs dimensionless shear rate for the Doi molecular model (calculations of Larson, ref 18). Regimes of positive and negative N_1 are indicated, as well as tumbling (T), wagging (W), and steady-state (S.S.) regimes. Open symbols represent time averages.

normal stress and order parameter calculations for a strength of the Onsager nematic potential, $U = 10.67$ (the lowest value for which a wholly nematic phase is stable). The change from positive to negative N_1 occurs near the transition from tumbling to wagging, while the transition from wagging to steady-state flow alignment occurs near the most negative N_1 values. Note that the tumbling and wagging regimes, the open symbols represent time averages over the periodic response. The squares show the anisotropy in the order parameter tensor relevant to our experimental studies, $S_{11} - S_{33}$. For a monodomain oriented along the 1-axis in the absence of flow, this quantity would take on the value $S^{eq} = 0.792$ for potential strength $U = 10.67$.[18] In the low shear rate tumbling regime, the predicted anisotropy is roughly 80% of this value and independent of shear rate. This represents the reduction in time-averaged molecular orientation associated with the rotation of the director through the tumbling orbit. This rather large orientation reflects the nature of Jeffery orbits,[4,18] which tend to accumulate near the flow direction and then flip rapidly through the remainder of the orbit. An 80% reduction relative to a static monodomain may be taken to be a first estimate of the disruptive influence of tumbling on orientation at low shear rates; the polydomain model of Larson and Doi discussed in the next subsection develops a more explicit picture of the orientation state in the linear regime.

The onset of nonlinear effects is first associated with a perturbation in the scalar order parameter, S, as the director rotates through its orbit. Sharp reductions in S during part of the orbit ultimately account for the onset of negative N_1 (see for instance Figure 5 of ref 18). While $S_{11} - S_{33}$ does show a barely perceptible decrease at intermediate shear rates, the sharp reduction in molecular orientation is not apparent in this projection of the microscopic order parameter tensor. Eventually, an increase in $S_{11} - S_{33}$ is predicted as the shear rate increases through wagging and into the steady flow alignment regime. An interesting feature of the high shear rate behavior is that even at extremely high deformation rates, the molecular anisotropy is *less* than that which would be observed in a monodomain in the absence of any flow field. (Comparison with Figure 9 of ref 18 shows that this is not an artifact of the particular projection of the order parameter tensor discussed here; at high shear rates the average molecular orientation angle is very close to the flow direction.)

3.2. Linear Larson–Doi Polydomain Model. One challenge of modeling textured PLC solutions is that the mechanical response reflects a distribution of director orientations. Larson and Doi recently proposed a model for the rheology of textured PLC solutions in the linear, tumbling regime that averages the response of the material over a distribution of domain orientations.[14] The structural response of the material is expressed as a pair of evolution equations for a mesoscopic order parameter tensor, $\bar{\mathbf{S}}$ reflecting the average domain orientation state (the degree of molecular orientation is assumed to be unperturbed within a given domain), and l, a scaled variable proportional to the defect density in the material (l goes as $1/a^2$, where a is the average texture length scale):

$$\frac{\mathrm{d}}{\mathrm{d}t}\bar{\mathbf{S}} = \omega^{\mathrm{T}}\cdot\bar{\mathbf{S}} + \bar{\mathbf{S}}\cdot\omega + \lambda[{}^2/_3\mathbf{D} + \mathbf{D}\cdot\bar{\mathbf{S}} + \bar{\mathbf{S}}\cdot\mathbf{D} - 2\bar{\mathbf{S}}:\mathbf{D}(\bar{\mathbf{S}} + {}^1/_3\delta)] - \epsilon l\bar{\mathbf{S}} \quad (5)$$

$$\frac{\mathrm{d}}{\mathrm{d}t}l = II_{\mathrm{D}}l - l^2 \quad (6)$$

In these expressions, $\mathbf{D}$ is the rate of deformation tensor, II_{D} is its second invariant, ω is the vorticity tensor, λ is the "tumbling parameter" (given as a function of concentration by the linearized Doi model analysis of Kuzuu and Doi[27]), and ϵ is an elasticity parameter. All but the final term on the right-hand side of eq 5 account for the hydrodynamic torques promoting tumbling, averaged over the domain distribution, the final term phenomenologically accounts for distortional elastic torques and is seen to be proportional to the defect density. Equation 6 is written such that, at steady state, the defect density is directly proportional to the shear rate, thus incorporating the hypothesis of texture refinement. As a consequence, the relative magnitudes of the hydrodynamic and elastic terms in eq 5 do not depend on shear rate at steady state; this torque balance is solely determined by the parameter ϵ, which is thus analogous to one over the saturation Ericksen number hypothesized by Burghardt and Fuller[5] and which determines the magnitude of strain recovery in recoil calculations and the persistence of oscillatory responses in transient flows (see the accompanying paper for a more detailed discussion of transient behavior[24]).

As a result of the scaling behavior implicit in the model's construction, its steady-state predictions for the mesoscopic order parameter components (and hence degree of orientation) are *independent of shear rate*; only the texture length scale changes with shear rate according to (6). Larson and Doi did not present the steady-state predictions of their model; these results are easily obtained by setting the time derivatives in eq 5 and 6 to zero (a cubic equation results for $\bar{S}_{12}$, from which the remaining mesoscopic order parameter components may be determined). Figure 2a shows the predicted anisotropy $\bar{S}_{11} - \bar{S}_{33}$ relevant to our studies, while Figure 2b shows the average domain orientation angle in the shear plane, $\bar{\chi}$, defined as

$$\bar{\chi} = \tan^{-1}\left[\frac{2\bar{S}_{12}}{\bar{S}_{11} - \bar{S}_{22}}\right] \quad (7)$$

These predictions are shown over the range of dimensionless concentration and elasticity parameter that result in good qualitative predictions of transient phenomena.[14] If all domains were oriented along the flow direction, $\bar{S}_{11} - \bar{S}_{33}$ would equal 1; the model therefore predicts that the birefringence observed under flow in the linear regime should be in the range of 80–90% of that observed in a monodomain in the absence of flow. Figure 2b shows that the domains are on average oriented very close to the flow direction. When the director is oriented along the flow direction, hydrodynamic torques are minimized; consequently, the steady-state domain orientation distribution function favors this configuration, resulting in this high degree of orientation (similar considerations account for the accumulation of unperturbed tumbling orbits along the flow direction; see section 3.1). However, the detailed steady-state structure depicted in Figure 2 also reflects the structure of eq 5 and in particular the phenomenological form of the elastic terms. In this paper, by combining birefringence measurements under flow with monodomain experiments, we are able to make quantitative tests of these predictions.

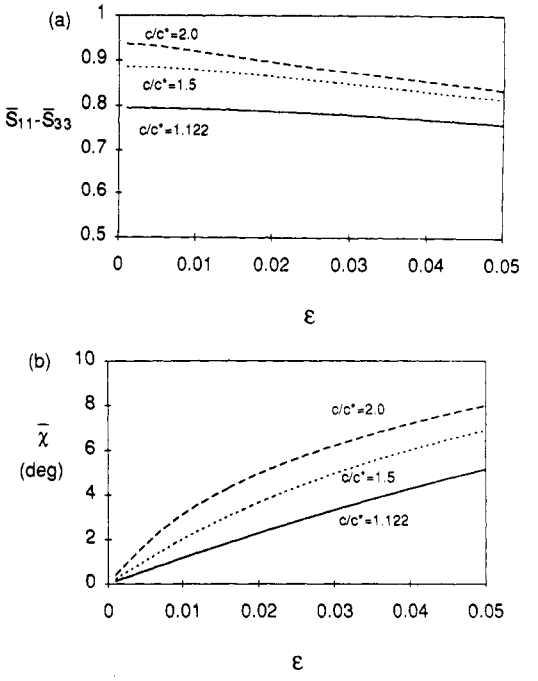

Figure 2. Larson and Doi model predictions of steady-state orientation in polydomain PLC's over a range of dimensionless concentration and elasticity parameter ϵ. (a) Anisotropy in the mesoscopic order parameter tensor $\bar{S}_{11} - \bar{S}_{33}$. (b) Average domain orientation angle, $\bar{\chi}$.

4. Experimental Section

4.1. Optical Analysis. For our birefringence measurements, we adapt the crossed and parallel polarizer arrangement used by Asada and co-workers.[21-23] The birefringent sample is placed between a polarizer and analyzer whose optical axes are either crossed or parallel to one another and at an orientation of ±45° with respect to the laboratory frame. The sample with birefringence Δn is assumed to be oriented with its principal axes at an angle θ. Analysis of this optical system yields the following expressions for the light intensity transmitted between crossed ($\perp$) and parallel ($\parallel$) polarizers:

$$I^{\perp} = \frac{I_0}{2}\mathrm{e}^{-2\alpha''}\sin^2(\pi\Delta n d/\lambda)\cos^2(2\theta) \quad (8)$$

$$I^{\parallel} = \frac{I_0}{2}\mathrm{e}^{-2\alpha''}[1 - \sin^2(\pi\Delta n d/\lambda)\cos^2(2\theta)] \quad (9)$$

In these expressions, the term $\mathrm{e}^{-2\alpha''}$ accounts for attenuation of light caused by scattering from the PLC texture, I_0 is the intensity of incident light with wavelength λ, and d is the sample thickness. The two experiments give complementary information, in that the sum $I^{\perp} + I^{\parallel}$ is independent of the anisotropic optical properties of the sample; normalizing the observed intensities with this sum removes the incident light intensity and any light atten-

uation from the analysis. We consequently present results in the normalized form:

$$N^{\perp} = \frac{I^{\perp}}{I^{\perp} + I^{\parallel}}; \quad N^{\parallel} = \frac{I^{\parallel}}{I^{\perp} + I^{\parallel}} \tag{10}$$

Equations 8 and 9 highlight the difficulties associated with crossed polarizer arrangements. The measured intensity depends on both the birefringence and optical orientation angle. This difficulty is often circumvented using more sophisticated polarization modulation techniques.[28] More important to the study of highly birefringent materials such as liquid crystals, the birefringence always appears as the argument of a sinusoidal function, so that data taken at a single wavelength cannot be uniquely inverted if the birefringence is large.

It has long been appreciated that the multiple-order difficulty may be circumvented through the use of polychromatic illumination, since according to eqs 8 and 9, different wavelengths will be extinguished at different values of Δn. This gives rise to the well-known interference colors exploited qualitatively in polarized microscopy of crystals.[29] More recently, Abetz and Fuller described a two-color polarization modulated flow birefringence apparatus that in particular resolves difficulties in orientation angle measurement as the retardation passes through multiple orders.[30] In this work, we avoid difficulties with multiple orders by measuring intensity as a function of wavelength through the visible spectrum. (A similar arrangement suitable for microscopic observation has recently been described by Boschmans.[31]) Equations 8 and 9 are then evaluated as functions of wavelength, where the birefringence determines the frequency with which maxima and minima are observed. The birefringence may be evaluated by fitting observed spectra to these equations. There is an additional wavelength dependence unaccounted for in these equations due to wavelength dispersion of the birefringence; this is discussed in detail in sections 4.3 and 5. Finally, we note that for highly birefringent materials, the determination of orientation angle is decoupled from the birefringence measurement, in that the latter is based on the wavelength dependence of transmitted light, allowing the former to be determined photometrically by absolute intensities. An illustration of this feature is provided in Figure 4.

The preceding analysis has neglected certain optical characteristics of sheared PLC solutions. For instance, all methods for birefringence measurement are also sensitive to linear dichroism. It is known that anisotropic light scattering from sheared PLC's gives rise to a conservative dichroism.[1,32] When dichroism is included in the analysis, $I^{\perp}$ becomes for the special case of $\theta = 0°$

$$I^{\perp} = \frac{I_0}{4} e^{-2\alpha''} [\cosh \delta'' - \cos(2\pi \Delta n d/\lambda)] \tag{11}$$

where the extinction $\delta'' = 2\pi \Delta n'' d/\lambda$ is defined in terms of the dichroism $\Delta n''$. Burghardt and Fuller observed a dichroism on the order of 10^{-5} in PBG solutions under shear.[1] Using values of $d = 1$ mm and $\lambda = 500$ nm relevant to our study, we find $\cosh \delta'' = 1.008$, which may be approximated as 1 within the accuracy of our measurements, yielding eq 8. More significant are the complications associated with polarization mixing alluded to in section 2. The light intensity transmitted between the polarizers will include contributions from a variety of light paths, each with its own characteristic spectrum. Thus there will be no true extinction at any wavelength, resulting in a reduction in the amplitude of the oscillations expected in $N^{\perp}$ and $N^{\parallel}$. We quantify these effects through an amplitude A, taken as the peak-to-peak variation in normalized intensity as a function of wavelength according to eqs 8–10. According to this definition, $A = 1$ for a sample behaving as an ideal retarder, while when $A = 0$, polarization mixing is so severe that there is no discernible difference between the measured spectra $I^{\perp}(\lambda)$ and $I^{\parallel}(\lambda)$.

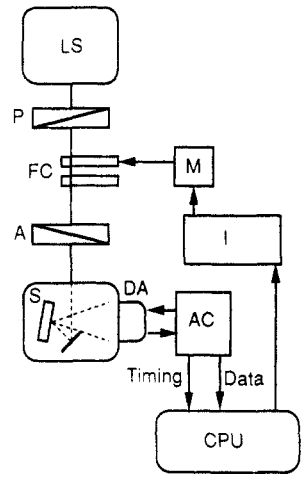

Figure 3. Schematic diagram of spectrographic birefringence experiment, showing light source (LS), polarizer (P), flow cell (FC), analyzer (A), spectrograph (S), diode array (DA), array controller (AC), motor (M), indexer (I), and computer (CPU).

4.2. Optical Train. A schematic illustration of the optical apparatus used in this work is shown in Figure 3. While light from a halogen source (Volpi Intralux 5000) is supplied to the optical train by a fiber optic guide, and then collimated with a lens. The light passes through a polarizer oriented at 45° with respect to the flow direction, the flow cell, and then through an analyzer which may be oriented either perpendicular or parallel to the polarizer. The flow cell consists of two parallel optical windows, separated by a gap of roughly 1 mm. Rotation of the lower plate is controlled by a computerized microstepping motor (Compumotor 4000 Indexer). Light is collected into a fiber optic cable and imaged onto the entrance slit of a grating spectrograph (Oriel MultiSpec), where the spectrum is projected onto a photodiode array (Reticon T series). Trigger and clock pulses from the diode array control circuit allow coordination of data acquisition so that one intensity value per pixel is collected for storage and subsequent analysis. Collection of an entire spectrum requires 20 ms; spectra are collected with both crossed and parallel polarizers for each birefringence measurement according to eqs 8–10.

An aperture above the flow cell and the entrance aperture of the fiber optic light collector define the light path through the flow cell. The measuring beam is displaced away from the axis of rotation, so that the flow field is locally simple shear, with the light propagating along the shear (2) axis. Thus, optical anisotropy in the flow–vorticity (1–3) plane is measured. It is difficult to glue windows into the flow cell in such a way that they are exactly parallel. In practice, there is roughly a 5% variation in the optical path length d (and hence also shear rate) as a function of the rotation of the flow cell. This is the major source of uncertainty in our measurements of birefringence (fitting spectra according to eqs 8–10 to determine the *product* of birefringence and path length, Δnd, is precise to the third significant digit). To minimize the effects of this uncertainty, all steady-state spectra are recorded at the same angular position of the flow cell.

4.3. Demonstration of Optical Technique. To test the apparatus and demonstrate the application of the

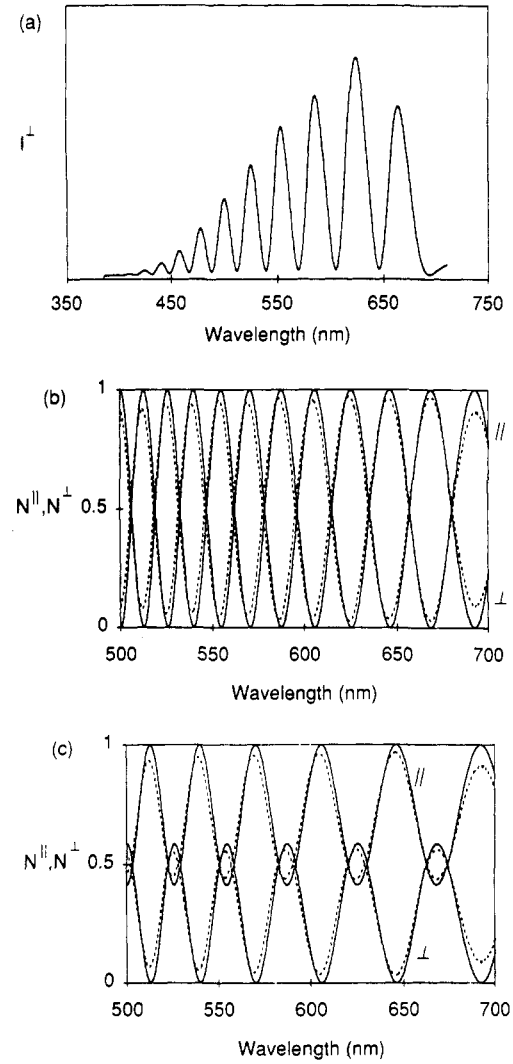

Figure 4. Optical data for known sample (multiple-order quartz quarter-wave plate). (a) Intensity transmitted between crossed polarizers vs wavelength; $\theta = 0°$, raw data. (b) Data for crossed and parallel polarizers normalized according to eq 10; $\theta = 0°$. (c) Normalized transmitted spectra for $\theta = 20°$.

spectrographic birefringence technique, measurements were made using a multiple-order quartz waveplate of known, large birefringence in place of the flow cell. Figure 4a shows the raw spectrum collected for crossed polarizers when the waveplate is placed with its optical axis along the flow direction ($\theta = 0°$). The intensity is an oscillatory function of wavelength, as suggested by eqs 8 and 9. The shape of the envelope reflects the spectrum of the incident light, the polarizers' transmission spectrum, and the diode array's spectral response. At short wavelengths, the light source emission spectrum weakens, while the cutoff at long wavelength is a consequence of a filter in the light source that protects the fiber optic guide from thermal damage. By normalizing the data according to eq 10, this wavelength dependence is removed. Figure 4b shows normalized experimental intensity spectra transmitted between crossed and parallel polarizers (dotted lines) along with the expected spectra based on the known optical properties (solid lines). A restricted wavelength range is presented for the sake of clarity. The experimental normalized spectra are seen to have an amplitude A slightly less than 1. This is due to a slight baseline offset in the photodiode array and does not reflect polarization mixing, which will be seen in Figures 6 and 7 to be significantly larger in sheared PLC solutions at low shear rates. This small baseline offset is seen to have no effect on the excellent agreement in the wavelength dependence of the normalized spectra (from which birefringence values are extracted), so we do not attempt any corrections to our data.

As noted in section 4.1, this technique is independently sensitive to optical orientation angle. As an example, Figure 4c shows experimental and calculated spectra for the waveplate when it is rotated to an angle $\theta = 20°$ with respect to the "flow" direction. The result of nonzero θ is a breaking of symmetry with respect to the normalized value of 0.5 in the spectra. In the current work, the symmetry imposed by the shear flow field dictates that $\theta = 0°$, as will be observed in subsequent sections.

The agreement between experiment and calculation in Figure 4 is only possible when the wavelength dispersion of the birefringence is properly taken into account. In this paper, we report birefringence values at the wavelength of 633 nm. The wavelength dependence of birefringence is approximated by the cubic relationship

$$\Delta n(\lambda) = \Delta n(633)[1 + ax + bx^2 + cx^3] \qquad (12)$$

where $x = (\lambda - 633)/633$ is a scaled wavelength and λ is the wavelength of light in nanometers. For the case of the quartz waveplate, the following values were obtained by fitting tabulated data in the visible range:[33] $a = -0.0677$, $b = 0.0713$, $c = -0.4606$, and $\Delta n(633) = 0.0090634$. This dispersion relationship was used along with eqs 8–10 to calculate the solid curves in Figure 4b,c.

4.4. Materials. In this work we have studied the model lyotropic PLC system of poly(γ-benzyl glutamate) (PBG) in m-cresol. Two concentrations of two molecular weights have been studied. Our high molecular weight sample consists of a closely matched racemic mixture combining equal weights of PBLG (Sigma lot 60h5512) and PBDG (Sigma lot 110h5531). We have measured the intrinsic viscosity of the racemic mixture to be 5.96 dL/g in m-cresol at 29 °C, corresponding to a viscosity-average molecular weight of 301 000, in good agreement with the values supplied by the manufacturer (310k for the PBLG and 298k for the PBDG). In addition, we have studied solutions of the single optical isomer, PBLG of lower molecular weight (Sigma lot 69f5501). We measured an intrinsic viscosity of 3.89 dL/g for this sample, corresponding to a viscosity-average molecular weight of 236 000. While PBLG solutions are cholesteric at rest, it is reported that they are transformed to nematics under shear flow due to the fragile cholesteric texture.[34] To the best of our knowledge, in all rheological investigations of poly(benzyl glutamate), there has been no distinction between the behavior of single optical isomers and racemic mixtures. However, use of a racemic mixture (which forms a simple nematic phase) is advantageous in the context of this work, in that oriented monodomains may be formed (see below). Solvent m-cresol (99%) was also purchased from Sigma; all materials were used as received. Two solution concentrations were studied, 13.5% and 20% PBG by weight, corresponding to 0.143 and 0.214 g/mL, respectively. Solutions were formed by weighing appropriate amounts of polymer and solvent into small bottles, sealing, and agitating periodically until homogeneous solutions were achieved (1–2 weeks). The PBG model system has been the object of extensive rheological and rheooptical studies. In particular, we note that the nematic solutions used here are quite similar to a solution for which director tumbling at low shear rates has been directly confirmed.[1]

4.5. Monodomain Formation. To form nematic PBG solution monodomains, we adapt a procedure described by Taratuta et al.[35] The sample is sandwiched between

two glass slides which have been coated with a hydrophobic hydrocarbon layer deposited from an ethylene plasma. It is hypothesized that this coating inhibits the otherwise observed tendency of PBG to adopt an end-on configuration at a glass surface, allowing for a parallel alignment. Uniform alignment is then induced by annealing the sample in a high-field (4.7 T) NMR magnet for a period of 24–48 h. All monodomains were checked for uniform orientation and an absence of texture in a polarizing optical microscope. The sample thickness is controlled by Teflon spacers and measured with a micrometer.

While it has been observed that monodomains prepared in this way persist for extended periods of time,[1,35] in the present case we observe disruption in the uniform orientation in a polarizing microscope, beginning several hours following removal of the sample from the magnet. The disruption generally begins at the boundaries with the Teflon spacer but sometimes also results from surface imperfections in the glass slides. We expect that the eventual loss of uniform orientation indicates that a true parallel boundary condition is *not* established at the hydrophobic surface of our substrates (such a boundary condition would act to maintain orientation despite perturbations at the edges). However, for the purposes of the present study, we only require that the monodomain be stable long enough for accurate and reproducible birefringence measurements. The monodomain birefringence values are extremely stable over the first several hours following removal of the sample from the magnet.

4.6. Mechanical Rheometry. Steady-shear viscosity and first and second normal stress difference measurements on several of the samples were performed on a modified R-17 Weissenberg rheogoniometer. This rheometer has been customized to measure the radial distribution of normal pressure in cone and plate flow, through the incorporation of four miniature flush-mounted capacitive pressure transducers. A radial momentum balance on homogeneous shear flow in a cone and plate geometry yields the following expression for the radial distribution of normal stress:[36]

$$-(\Pi_{22} + P_0) = -(N_1 + 2N_2)\ln(r/R) - N_2 \qquad (13)$$

Here Π_{22} is the component of the total stress tensor along the shear gradient (2) direction, P_0 is the atmospheric pressure, r is the radial position, and R is the radius of the plate. The first and second normal stress differences are defined according to usual convention as $N_1 = \Pi_{11} - \Pi_{22}$ and $N_2 = \Pi_{22} - \Pi_{33}$. A semilogarithmic plot of normal stress against radial coordinate should yield a straight line, with slope equal to $-(N_1 + 2N_2)$. N_1 may be independently measured by total normal thrust measurements, allowing determination of N_2. Extrapolation of the normal stress to the rim $r = R$ provides an alternate means of determining N_2. Magda and co-workers have used this instrument extensively to study normal stresses in a variety of polymer solutions, including liquid crystalline poly(benzyl glutamate) solutions.[20,37,38] Measurements were made using 74-mm-diameter fixtures and the following cone angles: 13.5% PBG(301k), 0.065 rad; 13.5% PBLG(236k), 0.038 rad; 20% PBLG(236k), 0.038 rad. Inertial corrections were applied to normal stress measurements at high shear rates.[39] The viscosity data were supplemented with steady-shear viscosity measurements of both the 13.5% and 20% PBG solutions using a Bohlin VOR rheometer, employing a cone and plate geometry with a 2.5° cone angle and 30-mm-diameter fixtures.

Figure 5 shows steady-state viscosity of the test solutions. The steady-shear viscosity behavior is in line with reported data on similar systems. The Newtonian plateaus below shear rates of around 1 s^{-1} are generally taken to be indicative of a linear regime in which nonlinear viscoelastic effects are negligible, while shear thinning at higher shear rates is believed to reflect nonlinear effects on the microscopic degree of molecular orientation. The "hesitation" in the viscosity curves in the shear-thinning region appears to be closely associated with the unusual normal stress behavior in these solutions and is predicted by theory.[20] At the relatively low polymer concentrations used here, there is no strong indication of so-called "region I" shear thinning at low deformation rates.[40]

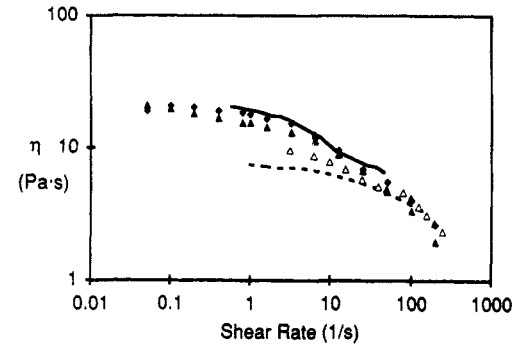

Figure 5. Steady shear viscosity vs shear rate: 13.5% PBG(301k) (—); 13.5% PBG(301k), VOR (◆); 20% PBG(301k), VOR (▲); 13.5% PBLG(235k) (△); 20% PBLG(236k) (- - -).

Table I
Birefringence in Nematic PBG Monodomains[a]

	Δn(633)	
thickness (μm)	13.5% PBG	20% PBG
146	0.00345	0.00570
146	0.00330	0.00565
277	0.00380	0.00615
858	0.00354	0.00603
av	0.0035 ± 0.0002	0.0059 ± 0.0003

[a] Dispersion coefficients: $a = -0.11$, $b = 0.18$, $c = -1.0$.

5. Monodomain Birefringence

Monodomains of various thicknesses were prepared according the procedure of section 4.5 and placed in the optical train aligned with $\theta = 0°$. To determine the birefringence, spectra were collected with crossed and parallel polarizers, and curves of $N^{\perp}$ and $N^{\parallel}$ were fitted to eqs 8–10 along with the dispersion relationship (12), using the birefringence as a fitting parameter. The coefficients a, b, and c in the dispersion relationship were adjusted to optimize the agreement between calculation and experiment. This procedure was complicated by ambiguity in fitting the data. Specifically, for a given monodomain thickness, there were multiple combinations of dispersion coefficient sets (a, b, c) and birefringence values $\Delta n(633)$ that would fit the curves adequately. This was particularly troublesome for thicker samples, where many maxima are observed in plots of $N^{\perp}$ and $N^{\parallel}$ wavelength. To determine the correct value of $\Delta n(633)$, a series of monodomains of various thicknesses were prepared. As the thickness was reduced, the number of "acceptable" dispersion relationships diminished, until only a single parameter set could be found that consistently fit all of the data; these parameters were the same for the 13.5 and 20% solutions.

Table I presents the birefringence observed for monodomains of various thicknesses for the two solutions as well as the dispersion coefficients determined by the above procedure. The average values of 0.0032 (±0.0002) and

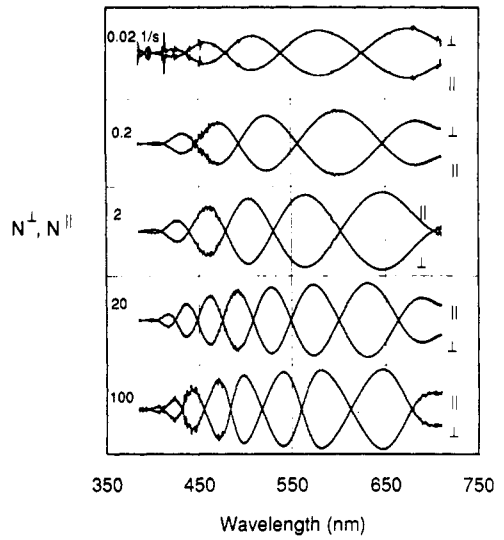

Figure 6. Normalized transmitted intensity spectra between crossed and parallel polarizers for sheared 13.5% PBG(301k) solution at indicated shear rates. For each shear rate, ordinate varies from 0 to 1 between gridlines.

0.0059 (±0.0003) for the two solutions are in reasonable agreement with published data of DuPre and Lin for similar solutions.[41] In the absence of data on Δn_0, the maximum birefringence attainable with perfect molecular alignment, we cannot use these values to evaluate the equilibrium order parameters according to eq 2. However, we can check for self-consistency in our measurements. Assuming that Δn_0 is proportional to polymer concentration, eq 2 allows us to calculate the ratio

$$\frac{S^{eq}(20\%)}{S^{eq}(13.5\%)} = \frac{0.0059}{0.0035}\frac{0.143}{0.214} = 1.13$$

indicating a slight increase in the degree of orientation with increased concentration. This result is consistent with previous measurements of the order parameter in PBG solutions[42] but is in contrast to recent measurements of birefringence in poly(*p*-phenylenebenzobisthiazole) (PBT) solutions that suggest an order parameter that is independent of concentration.[43]

6. Steady-Shear Results

It is well known that PBG solutions must be sheared through large strains to obtain reliable mechanical and rheooptical data.[44] All of our steady-state data have been obtained following application of shear strains of at least 200 strain units. Figure 6 presents spectra of transmitted light between crossed and parallel polarizers, normalized according to eq 10, for steady-shear flow of the textured 13.5% nematic PBG solution at a variety of shear rates. Similar spectra are observed for the remaining solutions. The spectra exhibit behavior in excellent qualitative agreement with the predictions of eqs 8–10, showing an oscillatory dependence on wavelength, with parallel and perpendicular spectra exactly out of phase. Furthermore, the spectra are observed to oscillate symmetrically about the value 0.5, indicating that the observed optical anisotropy is oriented along the flow direction (compare with Figure 4b,c). As the shear rate is increased, all solutions show an increasing number of oscillations, indicative of an increasing birefringence.

In section 2 we discussed some of the complications in interpreting measured optical properties in textured polymer liquid crystals. Equations 8–10 assume that the optical properties of the sheared PLC may be represented as a pure retarder. We may immediately recognize from Figure 6 that this description is inadequate in that the oscillations in normalized intensity do not approach extreme values of 0 and 1. Nevertheless, the strong characteristic oscillatory dependence on wavelength may only be explained by anisotropy in the retardation of light; the optical properties of the sheared PLC are dominated by birefringence. Since the optical volume is very large compared to the texture length scale, we argue that the detailed "domain" structure does not affect our measurements and that instead the measured birefringence provides a smoothed out, average measure of molecular orientation in the spirit of the mesoscopic order parameter introduced by Larson and Doi.[14] In support of this, we note that the transmitted spectra are extremely stable with time, except for slight periodic fluctuations associated with misalignment of the plates. On the other hand, one expects that the orientation state at the texture length scale would be quite unsteady as individual domains are deformed by the shear flow (recent microscopic visualization of sheared PBG solutions by Larson and Mead support this outlook[11]). The fact that our "macroscopic" measure of orientation is extremely steady supports the hypothesis that details in structure at the texture length scale are smoothed out in our measurements.

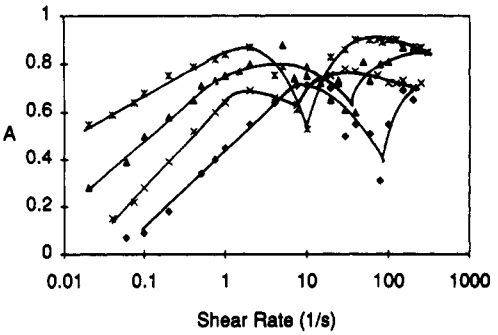

Figure 7. Amplitude of oscillations in normalized transmitted intensity spectra vs shear rate for 13.5% PBG(301k) (*), 13.5% PBLG(236k) (▲), 20% PBG(301k) (×), and 20% PBLG(236k) (◆). *A* is evaluated from data in the spectral range 600–650 nm.

Although polarization mixing does not interfere with the ability to extract birefringence values, it does provide some insight into the structural response of the sheared PLC solutions. Figure 7 shows the amplitude of the oscillations in the spectra of transmitted light (defined in section 4.1 as *A*) as a function of shear rate for the four solutions we have studied. At low shear rates, all solutions show an increase in *A* (that is, a *decrease* in polarization mixing) as the shear rate is increased. This observation is in general agreement with data of Asada and co-workers, who took it to be indicative of a refinement of the polydomain texture toward a more uniformly oriented state as the shear rate increased.[21,22] The two 13.5% solutions exhibit less polarization mixing than the 20% solutions, while at constant concentration less polarization mixing is observed in the higher molecular weight solutions. At higher shear rates the amplitude gets quite close to 1, indicating that the optical properties of the sheared PLC are close to those of an ideal retarder. However, several of the solutions exhibit a sharp drop in *A* over a narrow shear rate range, particularly evident in the 13.5% PBG(301k) and 20% PBLG(236k) solutions. This temporary reduction in *A* does not appear to be an artifact, as the raw birefringence data are extremely reproducible, including the amplitude of the oscillations. We will comment further on Figure 7 in our discussion section.

At any particular shear rate, spectra such as those observed in Figure 6 may be fit to eqs 8–10 in conjunction

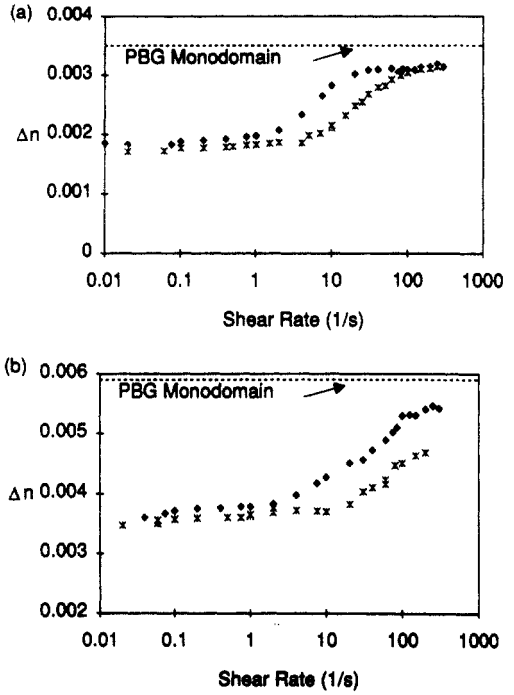

Figure 8. Steady-state birefringence vs shear rate: (a) 13.5% solutions; (b) 20% solutions. Racemic PBG(301k) (◆), PBLG-(236k) (*). Dashed lines give birefringence of PBG(301k) monodomains.

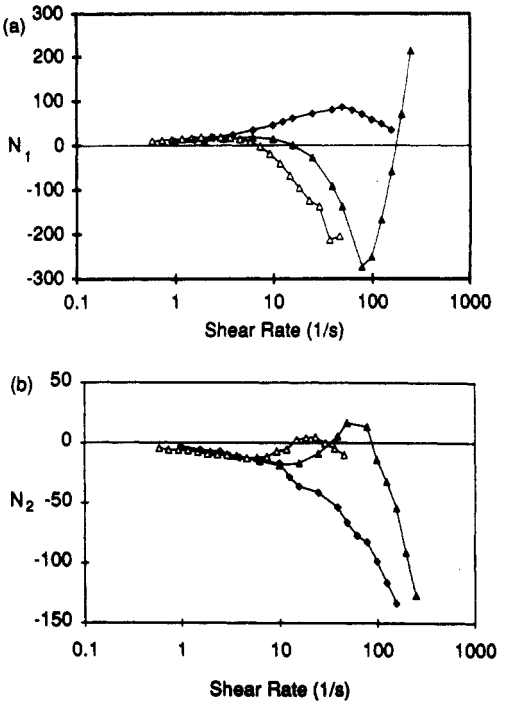

Figure 9. (a) First normal stress difference vs shear rate. (b) Second normal stress difference vs shear rate. 13.5% PBG(301k) (△); 13.5% PBLG(236k) (▲); 20% PBLG(236k) (◆).

Table II
Transition Shear Rates in Poly(benzyl glutamate) Solutions

sample	concn (wt %)	birefringence (s^{-1})	N_1 (+ to −) (s^{-1})
PBLG(236k)	13.5	23	16
	20	136	155–195
PBG(301k)	13.5	6	7
	20	32	

with the dispersion relationship (12) to evaluate the birefringence Δn at λ = 633 nm. The dispersion coefficients determined for PBG monodomains provide an excellent fit of the wavelength dependence of the spectra for all of the textured solutions studied under shear. Results are presented in Figure 8a for the two 13.5 wt % solutions and in Figure 8b for the two 20 wt % solutions. Note that these figures also show the birefringence of the perfectly oriented PBG (MW = 301k) monodomains. Naturally, the monodomain birefringence should properly be compared only with the shear flow data on the high molecular weight racemic sample.

The basic pattern of behavior is the same for all solutions studied. At low shear rates, the birefringence is essentially constant. For each concentration, the low shear rate birefringence for the 236k PBLG solution is slightly below that observed for the 301k PBG solution. As the shear rate is increased, there is an abrupt increase in the birefringence, whereupon the birefringence appears to become essentially constant again at high shear rates. The high shear rate plateau is most evident in the 13.5% PBG-(301k) solution, and there are indications of it in the 13.5% PBLG(236k) and 20% PBG(301k) solutions as well. However, our flow cell could not access sufficiently high shear rates to confirm a high shear rate plateau in the 20% PBLG(236k) solution. Figure 8 demonstrates that the shear rate at which this transition occurs increases with decreasing polymer molecular weight at both solution concentrations. In addition, by comparing parts a and b of Figure 8, it is clear that the transition shear rate increases with increasing polymer concentration as well. We quantify the transition shear rate as that for which the birefringence is roughly halfway between the high and low shear rate limits (0.0025 for the 13.5% solutions and 0.0046 for the 20% solutions). These transition shear rates are summarized in Table II.

Focusing on the behavior of the high molecular weight racemic PBG solutions at low shear rates, we observe that the measured birefringences of the 13.5 and 20% solutions are respectively 53 and 63% of those observed in quiescent, perfectly oriented monodomains. At high shear rates the birefringence is much higher, although still less than that observed in the monodomain (roughly 90% of the monodomain value).

Figure 9 shows the steady-state normal stress differences of three of the solutions under consideration. The general behavior pattern agrees with previous measurements of normal stresses in poly(benzyl glutamate) solutions.[20,38] N_1 and N_2 are both oscillatory functions of shear rate. The existence of a region of negative N_1 was first observed some time ago by Kiss and Porter,[44] but a corresponding region of positive N_2 was first observed only recently.[20] As the polymer concentration is increased, the onset of "interesting" normal stress behavior is shifted toward higher shear rates, consistent with the predictions of the Doi molecular model.[20] Here, too, we note that the transition from positive to negative first normal stress difference (which corresponds roughly to the location of the relative minimum in N_2) occurs at higher shear rate for the 20% PBLG(236k) solution than the 13.5% PBLG-(236k) solution. At a constant concentration of 13.5%, the high molecular weight (301k) solution exhibits behavior qualitatively similar to that of the lower molecular weight solution (236k), except that the normal stress transitions are shifted to lower shear rates. To characterize the trends with polymer concentration and molecular weight, we have summarized the shear rate at which N_1 first changes sign for the three solutions studied in Table II.

Magda and co-workers have extensively discussed the conditions under which reliable measurements of rheological properties may be obtained from cone and plate

flow.[20,38] In particular, for eq 13 to be valid it is necessary that the velocity field be macroscopically homogeneous, so that N_1 and N_2 are constant. Semilogarithmic plots of the radial distribution of normal stress will be linear if this condition is met. All of the measurements taken here satisfy this condition, in accord with previous experience.[20] At high shear rates, measurements are limited by the onset of an "edge fracture" instability that appears to be associated with a critical magnitude of the second normal stress difference.[45] In our case, this limit was reached for the two solutions of PBLG(236k). As a consequence of edge fracture in the 74-mm-diameter fixtures, the transition shear rate could not be precisely located for the 20% solution, and thus a range of shear rates is reported in Table II (normal thrust measurements with a 50-mm cone and plate fixture with a 0.0163-rad cone angle indicate a transition shear rate of 225 s^{-1}). Finally, for certain regions of shear rates, the normal stresses show time-dependent fluctuations.[38,46] Under these conditions, Figure 9 shows time-averaged values of the normal stress differences. As an example, the 13.5% PBG(301k) solution exhibits fluctuating values of N_1 for shear rates in the range $7.3 \leq \dot{\gamma} \leq 18.3$ s^{-1}, while steady values of N_1 are obtained for $\dot{\gamma} \leq 3.66$ and $\dot{\gamma} \geq 23.1$ s^{-1}.

7. Discussion

7.1. Linear Regime. It has been demonstrated that solutions of racemic PBG exhibit director tumbling in the linear limit.[1] The similarities in the rheological behavior of solutions of racemic PBG and PBLG, particularly regarding the "signature" phenomena believed to be associated with tumbling (for example, oscillatory responses in stress and structure in transient flows, large amounts of strain recovery at low shear rates, and the occurrence of negative N_1), lead us to adopt the hypothesis that tumbling is a general phenomenon in all lyotropic solutions of poly(benzyl glutamate) in *m*-cresol. In the low shear rate limit, it is expected that director tumbling will have a disruptive influence on the macroscopic orientation state in the material, due to the tendency toward director *rotation* rather than alignment. Comparison between the quiescent monodomain birefringence and that measured in textured solutions under shear flow provides a quantitative measure of the degree of disruption induced by tumbling.

We observe that the birefringence observed in the linear regime is in the range 53–63% of that seen in the monodomain for the two racemic PBG solutions. This is considerably below the predictions of around 80–90% associated with descriptions of director tumbling (see section 3). At the same time, these results indicate that there is a significant degree of molecular orientation that persists down to very low shear rates, in marked contrast to behavior in isotropic polymers. It has been suggested that at low shear rates, textured polymer liquid crystals exhibit a "piled polydomain" structure,[21] in which there would be negligible net molecular orientation as a result of the disruption induced by texture. This type of structure has been hypothesized to be associated with "region I" shear thinning at low shear rates.[40] Our shear viscosity data show no indication of region I behavior (Figure 5), so it appears that this regime is not present from either a structural or rheological point of view for the solutions under consideration. Region I shear thinning in PBG solutions is generally associated with higher solution concentrations than we have investigated;[21] further work is needed to elucidate possible connections between region I shear thinning and structure under flow.

While tumbling models overpredict the degree of orientation, the fact that the birefringence is found to be independent of shear rate in the linear regime is entirely consistent with the Larson and Doi model (section 3.2). According to this model, the texture length scale is refined by increasing shear rate in the linear regime in such a way that there is a rate-independent balance of hydrodynamic torques (tumbling) and distortional elastic torques which determines the steady-state domain orientation distribution function. Thus, the birefringence should be independent of shear rate. [Note that simple time averaging of a linear tumbling orbit leads to the same conclusion (section 3.1), since the orbit trajectory is independent of shear rate.] It is useful to recall scattering-induced dichroism data of Burghardt and Fuller (Figure 4 of ref 1) that indicate *substantial* changes in the texture length scale on very similar PBG solutions within the shear rate range for which Figure 8 indicates virtually *no* change in the degree of molecular orientation. Similarly, Figure 7 shows large changes in the polarization mixing induced by the texture within the low shear rate plateau of constant birefringence. Direct microscopic observation supports the hypothesis of texture refinement in the linear regime.[10,11] As the texture length scale decreases, averaging of the optical properties along a given light path will become more effective. This will reduce variability from one light path to another, resulting in less polarization mixing. In light of these complementary rheooptical data, the combined predictions of a constant degree of orientation and texture refinement may be taken to be a major success of the Larson–Doi model.

The interpretation of polarization mixing effects in terms of texture refinement is consistent with the discussion of Asada and co-workers.[21,22] While we are in substantial agreement with their conclusions regarding texture refinement, we are led to a different physical picture of textured PLC solutions at low shear rates. At low shear rates, Asada and co-workers observed significant polarization mixing along with an absence of oscillations as a function of shear rate in the light intensity transmitted between crossed and parallel polarizers (at a *single* wavelength; see, for instance, Figure 8 of ref 21), from which they concluded that there was very little net orientation in the flow direction.[21,22] These observations formed the original basis of the piled polydomain hypothesis. In contrast, Figures 6 and 8 clearly show a substantial degree of molecular alignment at low shear rates. The fact that the birefringence is essentially constant explains the absence in oscillations in transmitted (monochromatic) light as a function of shear rate. We believe that this illustrates the advantages of the spectrographic technique employed here, in that our measured birefringence values are quantitative and unambiguous. Another, more profound illustration of this advantage is presented in the accompanying paper in the context of relaxation processes.[24]

Our data indicate that director tumbling in textured PLC's causes a greater reduction in the degree of orientation than that predicted by tumbling models. Here we discuss three possible explanations. One possibility is a failure of the hypothesis that the microscopic degree of orientation is unperturbed by the flow field at low shear rates. Marrucci has suggested that the constant hydrodynamic torques promoting rotation of the director will eventually introduce distortions in the director field so severe as to approach the molecular length scale.[48] In the presence of such severe distortions, the Frank (small curvature) theory of distortional elasticity will break down,

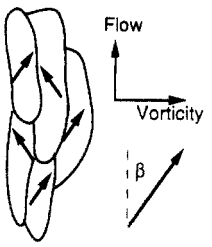

Figure 10. Schematic diagram of microscopic domain structure observed under flow by Larson and Mead.[11]

and it is reasonable to expect perturbations to the scalar order parameter S as well as the assumed uniaxial symmetry.[49] An analogous situation arises in the statics of liquid crystals, where Greco and Marrucci have calculated a reduction in molecular orientation caused by the high curvature imposed by a point disclination.[50] From eq 4 it is clear that any reduction in S due to distortional elastic effects in addition to reductions in $\bar{S}$ associated with tumbling would result in a lower than expected value of the birefringence. While the potential for severe distortions in the director field should be allowed, we do not believe these effects have influenced our measurements. Microscopic observations by Larson and Mead indicate that the texture length scale is on the order of 10 μm in PBG solutions sheared at low shear rates,[11] large enough that distortions so severe as to perturb S do not seem likely.

A second explanation for the discrepancy is that the qualitative idea of a continuous distribution of domain orientations may be too simplistic. Larson and Mead[11] have recently reported direct microscopic visualization of the detailed texture structure in very thin PBG samples under shear flow at low shear rates. Their observations suggest the existence of two discrete populations of director orientations, oriented at some angle, $\pm\beta$ (in the range of 35–45°) with respect to the flow direction, as shown in Figure 10. Crudely speaking, within any given "domain", the orientation flips back and forth between these two orientations as the director rotates in its tumbling orbit. The distribution of domain orientations remains symmetric with respect to the flow direction, so that on average the anisotropy is oriented along the flow direction, consistent with the symmetry observed in Figure 6. Since orbits which pass through the flow direction (and hence make the largest contribution to orientation in the 1–3 plane) do not appear to be present, this picture provides a natural explanation for a lower than expected macroscopic birefringence. These observations also suggest that considerably more structure needs to be built into polydomain models if they are to provide a qualitatively correct picture of the actual distribution of domain orientation distribution function under shear flow.

A final possibility regarding the lower than predicted birefringence in the linear regime relates to the projection of the refractive index tensor measured in our flow geometry. Both of the tumbling predictions of birefringence reflect the accumulation of tumbling orbits near the flow direction, resulting in an average domain orientation angle close to the flow direction (see Figure 2b for instance). If for some reason the average domain orientation angle χ was substantially larger than these models predict, the birefringence measured in our geometry would be lower than expected, without necessarily invoking a lower average degree of domain orientation $\bar{S}$. This circumstance is rather unlikely insofar as hydrodynamic torques on the director are minimized when the director is oriented in the 1–3 plane. Regardless of the possible perturbations to the tumbling orbits induced by distortional elasticity, it seems reasonable to expect that orientations in this plane would still be favored.

Before leaving the linear regime, we point out that there is a discrepancy between our observations on PBG solutions and the observations of Picken and co-workers on polyaramid solutions.[12] Refering back to our (qualitative) eq 4 and assuming that $S = S^{eq}$ in the low shear rate regime, the results in Figure 8 suggest that $\bar{S} \approx 0.53$–0.63 for our solutions. On the basis of X-ray scattering data, Picken and co-workers conclude that $\bar{S} \approx 1$ for all shear rates; they see no particular disruption in orientation associated with spatial variation of the director field (i.e., texture) in the low shear rate regime.[12] Since tumbling of liquid crystalline solutions of rodlike polymers at low shear rates has thus far proven to be the rule[1,2] and since some of the features of polyaramid rheology are reminiscent of tumbling (i.e., oscillatory responses in transient flows[12]), this discrepancy suggests at the least that the manifestations of tumbling may vary significantly from one system to another. At the other extreme, in thermotropic PLC's, Viola and Baird have shown by X-ray scattering that shear flow induces very little average molecular orientation.[51]

7.2. Nonlinear Regime. The remarkable rheological behavior of liquid crystalline polymer solutions in the nonlinear regime observed experimentally and qualitatively predicted by the Doi molecular model is believed to result from complex interactions between shear flow and the probability distribution function describing the orientation state of the constituent macromolecules. Our measurements of flow birefringence and normal stresses in sheared solutions of poly(benzyl glutamate) provide insights into the microscopic origins of unusual normal stress phenomena in the nonlinear regime.

Although the origin of the onset of negative first normal stress differences is believed to be a sharp reduction in the microscopic order parameter as the director executes a tumbling orbit, the Doi model calculations shown in Figure 1 indicate that the particular projection of the order parameter tensor probed by our birefringence experiments would not be expected to reveal any obvious decrease in orientation along the flow direction. Indeed, Figure 8 shows a monotonic increase in birefringence with shear rate. However, unlike the predictions in Figure 1 which show a gradual increase in orientation as the shear rate increases in the nonlinear regime, Figure 8 reveals an abrupt increase in orientation within a narrow shear rate range. (Again, there is a discrepancy between this observation and the results of Picken and co-workers, who observe no dramatic change in molecular orientation in polyaramid solutions using X-ray scattering.[12]) We attribute this increase to a transition from tumbling at low shear rates to (eventually) steady flow alignment at high shear rates. This hypothesis is primarily supported by comparison between the birefringence data in Figure 8 and the normal stress data in Figure 9. According to the Doi model, the region of negative N_1 is expected to be correlated with the transition region from tumbling to flow alignment. Table II, which summarizes characteristic shear rates of transitions in the birefringence and normal stresses, shows that these transition shear rates are close to one another. Moreover, variations in concentration or molecular weight that result in systematic shifts of the transition shear rates are seen to affect both the birefringence transition and normal stress transition to a comparable extent. This demonstrates that these transitions share a common origin. Since Doi model calculations indicate that the characteristic normal stress

behavior reflects the transition from tumbling to flow alignment and since such a transition might be expected to result in an increase in orientation (the predictions in Figure 1 notwithstanding), it is logical to reach the conclusion that the increase in birefringence in Figure 8 directly reflects this transition. Using light scattering, Ernst and co-workers have observed a pronounced structural transition to a high orientation state at a shear rate between 1.81 and 9.06 s^{-1}, in a PBG solution very similar to our 20% 301k sample.[52] This is somewhat lower than the value of 32 s^{-1} in Table II, but in prior work on solutions of (hydroxypropyl)cellulose, Ernst and Navard were also able to associate structural transitions measured by light scattering with normal stress transitions.[53]

Figure 1 indicates that there should be no abrupt change in molecular orientation accompanying the transitions from tumbling to wagging to flow alignment. However, our results in the linear, tumbling regime show that simple averaging over tumbling orbits (the procedure used in Figure 1) substantially overpredicts the degree of orientation. As discussed above, the additional disruption may reflect a more structured distribution of domains in the tumbling regime, where individual domains are predominantly found to be misaligned significantly with the flow direction.[11] As the shear rate increases through the wagging regime, nonlinear effects are predicted to result in increasingly strong attractions of the director toward the shear plane.[54] Ultimately, in the steady-flow regime, nonlinear effects should strongly promote a homogeneous molecular orientation state within the shear plane. We believe, therefore, that above the transition to a highly oriented state, the predictions of Figure 1 should be relevant. Indeed, the observed birefringence of roughly 90% that of a quiescent monodomain is in reasonable agreement with Doi model predictions. An additional decrease in orientation induced by tumbling, not accounted for in Figure 1, suppresses the birefringence in the low shear rate regime, thus revealing the transition observed in Figure 8.

The dependence of the transition shear rates on concentration has been shown to be in excellent agreement with Doi model predictions in the context of studying normal stress behavior.[20] Here we additionally observe an effect of polymer molecular weight at constant concentration. As the molecular weight increases, the rotational diffusivity of the rodlike molecules will decrease, increasing the characteristic relaxation time of the solution, τ. Since the onset of the characteristic nonlinear behavior should occur at roughly the same Weissenberg number ($Wi = \dot{\gamma}\cdot\tau$), an increase in τ should shift the transition from tumbling to flow alignment to lower shear rates,[45] consistent with the observations in Figures 8 and 9.

In section 6 is was noted that over a certain narrow range of shear rates the normal stress signals exhibit time-dependent fluctuations. Magda and co-workers[20,38] have suggested that these fluctuations might correspond to the wagging regime predicted by the Doi model.[16-18] In our birefringence experiments we see no strong evidence of any time-dependent behavior in the corresponding shear rate range, although the slight misalignment of the two plates would tend to obscure any fluctuations in birefringence on the order of 5% or less of the steady value. If, as Magda and co-workers suggest, the fluctuations reflect some sort of "coherent" wagging within the macroscopically homogeneous cone and plate flow,[20] it is plausible that there would be little evidence of them in the macroscopically *inhomogeneous* parallel plate flow used in the optical experiments. However, it is interesting to note that the narrow "spike" observed in the polarization mixing behavior for the 13.5% PBG(301k) solution (Figure 7) occurs in a similar shear rate range, $4 \leq \dot{\gamma} \leq 20$ s^{-1} as the time-dependent fluctuations in normal stress measurements of the same solution, $7.3 \leq \dot{\gamma} \leq 18.3$ s^{-1}. This shear rate range does correspond roughly to the range in which wagging would be expected, based on comparisons between Figure 1 and Figure 9. It is possible that the wagging regime introduces some additional perturbation in the texture that results in a temporary increase in polarization mixing, until the steady flow alignment regime is reached. This outlook is in agreement with the observation of substantial fluctuations in scattering-induced dichroism associated with texture by Moldenaers and co-workers in a shear rate range in which normal force oscillations were observed.[32] Furthermore, recent microscopic observations show a striking striped texture that appears within the expected wagging shear rate range.[55]

8. Conclusions

We have described a new flow birefringence apparatus that allows for unambiguous measurements of birefringence in materials of high optical anisotropy. This instrument was used to study the degree of molecular orientation of textured, liquid crystalline solutions of poly(benzyl glutamate) under shear flow. At low shear rates, the birefringence is constant, in the range of 53–63% of that measured in quiescent monodomains, although polarization mixing effects and previous rheooptical studies suggest substantial changes in the texture length scale in this shear rate range. No evidence of "region I" behavior was observed, either structurally or rheologically. The birefringence plateau at low shear rates is consistent with the known occurrence of director tumbling in these materials; however, tumbling models overpredict the degree of orientation in the low shear rate regime. We tentatively attribute this discrepancy to a more structured distribution of domain orientations in the low shear rate regime, as observed microscopically by Larson and Mead,[11] in which individual domains are misaligned with the flow direction.

A transition is observed in molecular orientation as the shear rate is increased, to a high shear rate regime where the birefringence is roughly 90% of that observed in a quiescent monodomain. This degree of orientation is consistent with Doi model predictions in the nonlinear steady-flow alignment regime. This transition is closely coupled to the change in sign of the first normal stress difference and is consequently taken to be a manifestation of a transition from tumbling to flow alignment. The dependence of this transition on concentration and molecular weight is consistent with Doi model predictions.

Acknowledgment. We gratefully acknowledge the assistance of many colleagues in the preparation of this work. The construction and testing of the optical train in Figure 3 were initiated by a Master's student at Northwestern, Aulia, currently employed by Procter and Gamble in Cincinnati. We thank Dr. R. G. Larson for providing the 236k PBLG sample, the detailed results of nonlinear Doi model calculations presented in Figure 1, and many helpful discussions. Dr. K. Amundson is acknowledged for a helpful discussion regarding birefringence in textured media. We also thank Dr. C. Herb for access to the Bohlin VOR used for supplemental viscosity measurements. At Northwestern, Professor M. A. Petrich and Mr. R. Lu provided valuable assistance in the formation of monodomains (the NMR magnet used for

monodomain preparation was purchased under NSF grant MSS-9007683). Financial support for this work was provided in part by the National Science Foundation (Grant CTS-9109898 at Northwestern and Grant CTS-9022734 at Utah) and by funds from the June and Donald Brewer Junior Professorship (W.R.B.). Finally, construction of the optical apparatus described in section 4.2 was partially supported by a grant from the Northwestern University Research Grants Committee.

References and Notes

(1) Burghardt, W. R.; Fuller, G. G. *Macromolecules* **1991**, *24*, 2546.
(2) Srinivasarao, M.; Berry, G. C. *J. Rheol.* **1991**, *35*, 379.
(3) Leslie, F. M. *Adv. Liq. Cryst.* **1979**, *4*, 1.
(4) Jeffery, G. B. *Proc. R. Soc. London, A* **1922**, *102*, 161.
(5) Burghardt, W. R.; Fuller, G. G. *J. Rheol.* **1990**, *34*, 959.
(6) Marrucci, G. *Pure Appl. Chem.* **1985**, *57*, 1545.
(7) Wissbrun, K. *Faraday Discuss. Chem. Soc.* **1985**, *79*, 161.
(8) Larson, R. G.; Mead, D. W. *J. Rheol.* **1989**, *33*, 1251.
(9) Alderman, N. J.; Mackley, M. R. *Faraday Discuss. Chem. Soc.* **1985**, *79*, 1.
(10) Gleeson, J. T.; Larson, R. G.; Mead, D. W.; Kiss, G.; Cladis, P. E. *Liq. Cryst.* **1992**, *11*, 341.
(11) Larson, R. G.; Mead, D. W. *Liq. Cryst.*, in press.
(12) Picken, S. J.; Aerts, J.; Doppert, H. L.; Reuvers, A. J.; Northolt, M. G. *Macromolecules* **1991**, *24*, 1366.
(13) Moldenaers, P.; Mewis, J. *J. Rheol.* **1986**, *30*, 567.
(14) Larson, R. G.; Doi, M. *J. Rheol.* **1991**, *35*, 539.
(15) Marrucci, G.; Maffettone, P. L. *Macromolecules* **1989**, *22*, 4076.
(16) Marrucci, G.; Maffettone, P. L. *J. Rheol.* **1990**, *34*, 1217.
(17) Marrucci, G.; Maffettone, P. L. *J. Rheol.* **1990**, *34*, 1231.
(18) Larson, R. G. *Macromolecules* **1990**, *23*, 3983.
(19) Doi, M. *J. Polym. Sci., Polym. Phys. Ed.* **1981**, *19*, 229.
(20) Magda, J. J.; Baek, S.-G.; DeVries, K. L.; Larson, R. G. *Macromolecules* **1991**, *24*, 4460.
(21) Asada, T.; Muramatsu, H.; Watanabe, R.; Onogi, S. *Macromolecules* **1980**, *13*, 867.
(22) Asada, T. In *Polymer Liquid Crystals*; Ciferri, A., Krigbaum, W. R., Meyer, R. B., Eds.; Academic Press: New York, 1982.
(23) Asada, T.; Onogi, S.; Yanase, H. *Polym. Eng. Sci.* **1984**, *24*, 355.
(24) Hongladarom, K.; Burghardt, W. R. *Macromolecules*, following paper in this issue.
(25) Doi, M.; Edwards, S. F. *The Theory of Polymer Dynamics*; Clarendon: Oxford, 1986.
(26) Amundson, K.; Helfand, E.; Patel, S. S.; Quan, X.; Smith, S. D. *Macromolecules* **1992**, *25*, 1935.
(27) Kuzuu, N.; Doi, M. *J. Phys. Soc. Jpn.* **1984**, *53*, 1031.
(28) Fuller, G. G. *Annu. Rev. Fluid Mech.* **1990**, *22*, 387.
(29) Gay, P. *An Introduction to Crystal Optics*; Longmans: London, 1967.
(30) Abetz, V.; Fuller, G. G. *Rheol. Acta* **1990**, *29*, 11.
(31) Boschmans, M. *Mol. Cryst. Liq. Cryst.* **1991**, *199*, 267.
(32) Moldenaers, P.; Fuller, G. G.; Mewis, J. *Macromolecules* **1989**, *22*, 960.
(33) *Handbook of Optical Constants of Solids*; Palik, E. D., Ed.; Academic Press: Oxford, 1985; pp 728–9.
(34) Kiss, G.; Porter, R. S. *J. Polym. Sci., Polym. Phys. Ed.* **1980**, *18*, 361.
(35) Taratuta, V. G.; Srajer, G. M.; Meyer, R. B. *Mol. Cryst. Liq. Cryst.* **1985**, *116*, 245.
(36) Bird, R. B.; Armstrong, R. C.; Hassager, O. *Dynamics of Polymeric Liquids, Fluid Mechanics*; Wiley: New York, 1987; Vol. 1.
(37) Magda, J. J.; Lou, J.; Baek, S.-G.; DeVries, K. L. *Polymer* **1991**, *32*, 2000.
(38) Magda, J. J.; Baek, S.-G.; DeVries, K. L.; Larson, R. G. *Polymer* **1991**, *32*, 1794.
(39) Turian, R. M. *Ind. Eng. Chem. Fundam.* **1972**, *11*, 361.
(40) Onogi, S.; Asada, T. In *Rheology*; Astarita, G., Marrucci, G., Nicolais, L., Eds.; Plenum Press: New York, 1980.
(41) DuPre, D. P.; Lin, F. M. *Mol. Cryst. Liq. Cryst.* **1981**, *75*, 217.
(42) Murth, N. S.; Knox, J. R.; Samulski, E. T. *J. Chem. Phys.* **1976**, *65*, 4835.
(43) Mattoussi, H.; Srinivasarao, M.; Kaatz, P. G.; Berry, G. C. *Macromolecules* **1992**, *25*, 2860.
(44) Mewis, J.; Moldenaers, P. *Mol. Cryst. Liq. Cryst.* **1987**, *153*, 291.
(45) Kiss, G.; Porter, R. S. *J. Polym. Sci., Polym. Phys. Ed.* **1978**, *65*, 193.
(46) Baek, S.-G.; Magda, J. J.; Cementwala, S.; Larson, R. G.; Grizutti, N. In *Theoretical and Applied Rheology*; Moldenaers, P., Keunings, R., Eds.; Elsevier: Amsterdam, 1992; p 516.
(47) Moldenaers, P. Doctoral Dissertation, Katholieke Universiteit Leuven, 1987.
(48) Marrucci, G. *Macromolecules* **1991**, *24*, 4176.
(49) Greco, F.; Marrucci, G. *Mol. Cryst. Liq. Cryst.* **1992**, *212*, 125.
(50) Greco, F.; Marrucci, G. *Mol. Cryst. Liq. Cryst.* **1992**, *210*, 129.
(51) Viola, G. G.; Baird, D. G. *J. Rheol.* **1986**, *30*, 601.
(52) Ernst, B.; Navard, P.; Hashimoto, T.; Takebe, T. *Macromolecules* **1990**, *23*, 1370.
(53) Ernst, B.; Navard, P. *Macromolecules* **1989**, *22*, 1419.
(54) Larson, R. G.; Ottinger, H. C. *Macromolecules* **1991**, *24*, 6270.
(55) Larson, R. G, personal communication, 1992.